

toxicity is due to the diatom culture conditions in the laboratory or that cases of toxicity are exceptions, owing to the species or strains maintained in laboratory cultures being unrepresentative of natural field populations.

However, any explanation for the discrepancy between the laboratory and field results does not affect our conclusion. The range of areas and copepod and diatom species considered in this study provide strong evidence that, under natural environmental conditions, there is no negative effect of diatoms on copepod hatching success. We conclude that there is no need to revise existing conceptual models of energy transfer from phytoplankton, through copepods, to fish in diatom-dominated systems. □

**Methods**

**Hatching success**

Eggs for the hatching success measurements were obtained from females incubated in filtered or natural sea water (depending on the species, some copepods stop spawning in filtered sea water) during the first 12–24 h after capture<sup>18</sup>. The intention was to minimise the effect of the incubation conditions to obtain hatching rates representative of the field values. From the egg production experiments 30–100 eggs were selected randomly and gently transferred to 60-ml tubes filled with filtered sea water. The samples were incubated, at sea surface temperature, for periods ranging from 48 to 96 h (depending on the temperature). After the incubation period, the samples were examined microscopically to determine the number of nauplii and unhatched eggs.

**Microplankton identification and biomass**

Water samples for identification of microplankton (>2 µm, nanoplankton plus microplankton) species and carbon estimation were collected generally at the chlorophyll maximum depth and preserved with 1% final concentration of Lugol's iodine solution<sup>19</sup>. Subsamples (100 ml) were settled (Utermöhl technique) and counted with an inverted microscope. Phytoplankton carbon biomass was estimated from cell volume<sup>20</sup> and using a factor of 0.21 pg C µm<sup>-3</sup> (ref. 21) for ciliates. Heterotrophic dinoflagellates were separated from autotrophic forms according to taxonomic considerations<sup>22</sup>.

Received 19 April; accepted 15 July 2002; doi:10.1038/nature01055.

1. Miralto, A. *et al.* The insidious effect of diatoms on copepod reproduction. *Nature* **402**, 173–176 (1999).
2. Ban, S. *et al.* The paradox of diatom-copepod interactions. *Mar. Ecol. Prog. Ser.* **157**, 287–293 (1997).
3. Uye, S. Induction of reproductive failure in the planktonic copepod *Calanus pacificus* by diatoms. *Mar. Ecol. Prog. Ser.* **133**, 89–97 (1996).
4. Paffenhöfer, G.-A. An assessment of the effects of diatoms on planktonic copepods. *Mar. Ecol. Prog. Ser.* **227**, 305–310 (2002).
5. Cushing, D. H. A difference in structure between ecosystems in strongly stratified waters and in those that are weakly stratified. *J. Plankton Res.* **11**, 1–13 (1989).
6. Legendre, L. The significance of microalgal blooms for fisheries and for the export of particulate organic carbon in oceans. *J. Plankton Res.* **12**, 681–699 (1990).
7. Runge, J. A. Should we expect a relationship between primary production and fisheries? The role of copepod dynamics as a filter of trophic variability. *Hydrobiologia* **167/168**, 61–71 (1988).
8. Ohman, M. D. & Hirche, H.-J. Density-dependent mortality in an oceanic copepod population. *Nature* **412**, 638–641 (2001).
9. Pauly, D. & Christensen, V. Primary production required to sustain global fisheries. *Nature* **374**, 255–257 (1995).
10. Ianora, A., Miralto, A. & Poulet, S. A. Are diatoms good or toxic for copepods? Reply to comment by Jónasdóttir *et al.* *Mar. Ecol. Prog. Ser.* **177**, 305–308 (1999).
11. Jónasdóttir, S. H. *et al.* Role of diatoms in copepod production: good, harmless or toxic? *Mar. Ecol. Prog. Ser.* **172**, 305–308 (1998).
12. Poulet, S., Ianora, A., Miralto, A. & Meijer, L. Do diatoms arrest embryonic development in copepods? *Mar. Ecol. Prog. Ser.* **111**, 79–86 (1994).
13. Ianora, A., Poulet, S. A., Miralto, A. & Grottolli, R. The diatom *Thalassiosira rotula* affects reproductive success in the copepod *Acartia clausi*. *Mar. Biol.* **125**, 279–286 (1996).
14. Pohner, G. Wound-activated chemical defense in unicellular planktonic algae. *Angew. Chem. Int. Edn* **39**, 4352–4354 (2000).
15. Peterson, W. T. Patterns in stage duration and development among marine and freshwater calanoid and cyclopoid copepods: a review of rules, physiological constraints, and evolutionary significance. *Hydrobiologia* **453/454**, 91–105 (2001).
16. Irigoien, X. *et al.* Feeding selectivity and egg production of *Calanus helgolandicus* in the English Channel. *Limnol. Oceanogr.* **45**, 44–54 (2000).
17. Irigoien, X., Harris, R. P., Head, R. N. & Harbour, D. The influence of diatom abundance on the egg production rate of *Calanus helgolandicus* in the English Channel. *Limnol. Oceanogr.* **45**, 1433–1439 (2000).
18. Runge, J. A. & Roff, J. C. *ICES Zooplankton Methodology Manual* (eds Harris, R., Wiebe, P. H., Lenz, J., Skjoldal, H. R. & Huntley, M. E.) 401–454 (Academic, London, 2000).
19. Holligan, P. M. & Harbour, D. S. The vertical distribution and succession of phytoplankton in the western English Channel in 1975 and 1976. *J. Mar. Biol. Assoc. UK* **57**, 1075–1093 (1977).
20. Strathmann, R. R. Estimating the organic carbon content of phytoplankton from cell volume or plasma volume. *Limnol. Oceanogr.* **12**, 411–418 (1967).
21. Ohman, M. D. & Runge, J. A. Sustained fecundity when phytoplankton resources are in short supply: omnivory by *Calanus finmarchicus* in the Gulf of St Lawrence. *Limnol. Oceanogr.* **39**, 21–36 (1994).
22. Lessard, E. J. & Swift, E. Dinoflagellates from the North Atlantic classified as phototrophic or heterotrophic by epifluorescence microscopy. *J. Plankton Res.* **8**, 1209–1215 (1986).

Supplementary Information accompanies the paper on Nature's website (<http://www.nature.com/nature>).

**Acknowledgements**

This is a contribution to the international GLOBEC (Global Ocean Ecosystem Dynamics) programme. We thank the captains and crews of the research vessels who made this work possible.

**Competing interests statement**

The authors declare that they have no competing financial interests.

Correspondence and requests for materials should be addressed to X.I. (e-mail: xirigoien@pas.azti.es).

**Epiparasitic plants specialized on arbuscular mycorrhizal fungi**

Martin I. Bidartondo\*†, Dirk Redecker†‡, Isabelle Hijri‡, Andres Wiemken‡, Thomas D. Bruns\*, Laura Dominguez§, Alicia Sérsic§, Jonathan R. Leake|| & David J. Read||

\* Department of Plant & Microbial Biology, University of California, Berkeley, California 94720-3102, USA  
 ‡ Institute of Botany, University of Basel, Hebelstrasse 1, 4056 Basel, Switzerland  
 § Instituto Multidisciplinario de Biología Vegetal, C.C. 495, Córdoba 5000, Argentina  
 || Department of Animal & Plant Sciences, University of Sheffield, Sheffield S10 2TN, UK  
 † These authors contributed equally to this work

Over 400 non-photosynthetic species from 10 families of vascular plants obtain their carbon from fungi and are thus defined as myco-heterotrophs<sup>1</sup>. Many of these plants are epiparasitic on green plants from which they obtain carbon by 'cheating' shared mycorrhizal fungi<sup>2–7</sup>. Epiparasitic plants examined to date depend on ectomycorrhizal fungi for carbon transfer and exhibit

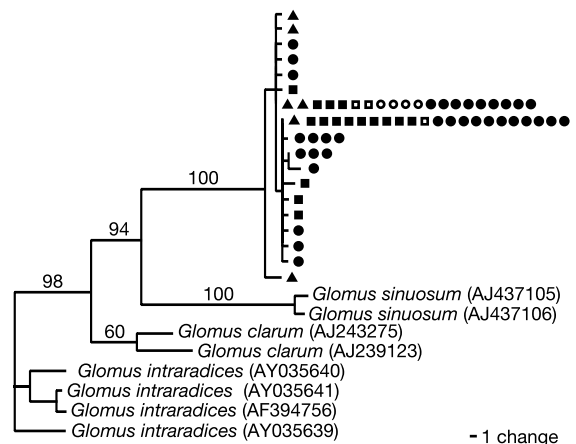


**Figure 1** The AMF of *Arachnitis* are markedly similar, showing minimal variation in the generally highly polymorphic internal transcribed spacers of nuclear DNA. The phylogenetic tree shows the placement of fungal sequences among their closest available alignable relatives. Identical sequences are represented by symbols in a row: filled triangles, circles, and squares correspond to fungal sequences obtained from root samples of *Arachnitis* from each of three locations (eight plants); open symbols correspond to fungal sequences obtained from adjacent root samples of green plants that are identical to sequences obtained from *Arachnitis* root samples. Neighbour-joining tree with 10,000 bootstrap replicates for 71 sequences and 442 characters. GenBank accession numbers are shown in parentheses.

exceptional specificity for these fungi<sup>3-7</sup>, but for most myco-heterotrophs neither the identity of the fungi nor the sources of their carbon are known. Because many myco-heterotrophs grow in forests dominated by plants associated with arbuscular mycorrhizal fungi (AMF; phylum Glomeromycota), we proposed that epiparasitism would occur also between plants linked by AMF. On a global scale AMF form the most widespread mycorrhizae, thus the ability of plants to cheat this symbiosis would be highly significant. We analysed mycorrhizae from three populations of *Arachnitis uniflora* (Corsiaceae, Monocotyledonae), five *Voyria* species and one *Voyriella* species (Gentianaceae, Dicotyledonae), and neighbouring green plants. Here we show that non-photosynthetic plants associate with AMF and can display the characteristic specificity of epiparasites. This suggests that AMF mediate significant inter-plant carbon transfer in nature.

Arbuscular mycorrhizal fungi (AMF) are nutrient-gathering obligate symbionts of most plant species. In contrast to the situation in the ectomycorrhizal symbiosis, the arbuscular mycorrhizal symbiosis lacks examples of absolute specificity and net fungus-to-plant carbon transfer<sup>3,8-10</sup>. Despite the widespread potential for inter-plant linkage offered by the generalist behaviour of AMF<sup>10-12</sup>, experimental evidence for inter-plant carbon transfer is equivocal because transferred carbon may remain in fungal structures within

roots and carbon flux between autotrophs may be bi-directional<sup>13,14</sup>. Consequently, it has been stated that in nature "there is no fungus-to-plant carbon transfer"<sup>14</sup>. However, by definition, net carbon transfer must occur from fungus to myco-heterotroph. Although in the ectomycorrhizal symbiosis myco-heterotrophs are extreme examples of both specialization and epiparasitism, evidence for these phenomena is lacking in putative arbuscular mycorrhizal myco-heterotrophs<sup>1,15,16</sup>.

We show that the non-photosynthetic plant *Arachnitis uniflora* from three subantarctic forest sites in Argentina forms arbuscular mycorrhizae and that it is specialized to a narrow lineage within a clade of *Glomus* (*Glomus* group A<sup>17</sup>). We were able to use universal fungal-specific primers to amplify and sequence the highly polymorphic nuclear ribosomal internal transcribed spacer (nrITS) region directly from *Arachnitis* roots. This in itself is unusual, because polymerase chain reaction (PCR) detection of AMF in green plants usually requires specific primers, nested amplifications, and cloning due to low template concentrations, inhibitors, and high complexity of root fungal communities. The sequences from all eight specimens were nearly identical. To verify the absence of other mycorrhizal fungi, we cloned and sequenced from the direct amplicon pools of all specimens (Fig. 1). The nrITS sequences obtained show a polymorphism that is within the range of intra-

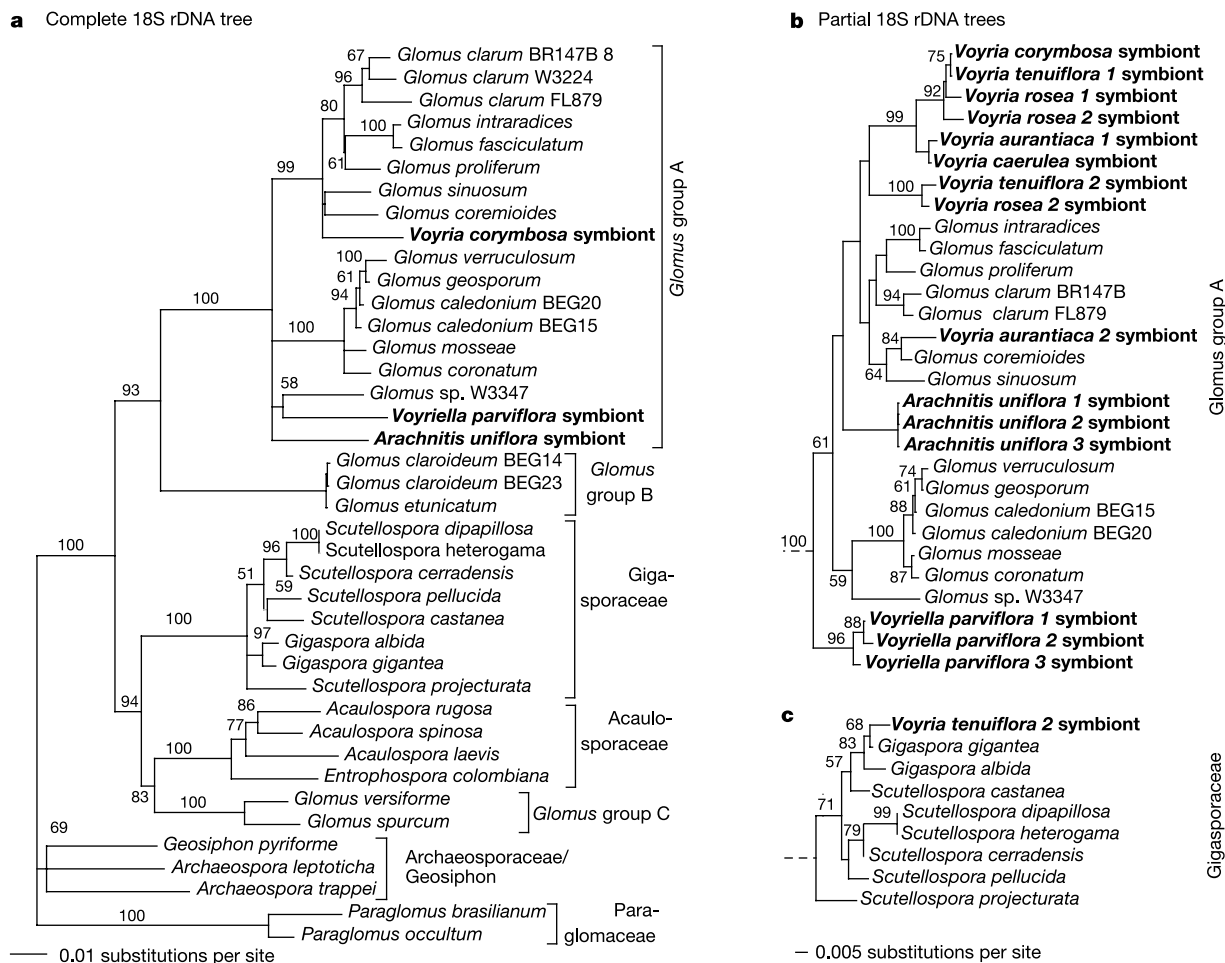


**Figure 2** Most of the arbuscular mycorrhizal symbionts of the three plant genera sampled fall into three distinct clades within *Glomus* group A. **a**, Phylogenetic tree using complete 18S nuclear DNA sequences from all known families and lineages of AMF and a subset of myco-heterotroph symbionts. Neighbour-joining tree using 1,611 characters. Nodes with bootstrap values below 50 were collapsed to polytomies. **b**, *Arachnitis* AMF are found only in one narrow clade of *Glomus* group A. Three of eight nearly identical AMF 18S nuclear DNA sequences obtained from three plants are shown here, one from each site sampled.

*Voyriella* AMF are restricted to another *Glomus* group A lineage, whereas *Voyria* spp. have the most diverse set of AMF within *Glomus* group A. Neighbour-joining tree with 1,000 bootstrap replicates using 450 characters from the 3'-terminal region of the 18S. *Glomus* group B was used as an outgroup. **c**, The only detected *Voyria* symbiont not in *Glomus* group A is in the Gigasporaceae. This tree was obtained as in **b**, with *Acaulospora laevis* used as an outgroup.

species or intra-spore variation in AMF<sup>18</sup>. The *Glomus* lineage detected in *Arachnitis* also formed mycorrhizae in adjacent photosynthetic plants from three different families (Fig. 1); these or other co-occurring plants must be the ultimate sources of carbon for *Arachnitis*, as AMF are not saprotrophs. The plant roots were identified morphologically or by nrITS sequence similarity to GenBank accessions or leaves obtained at the sites: *Osmorhiza chilensis* (Apiaceae) (AF480090), *Austrocedrus chilensis* (Cupressaceae), and *Nothofagus dombeyi* (Nothofagaceae) (AF480091, AF480092). We detected three other AMF lineages in the vicinity of *Arachnitis* roots but not associated with them, indicating that plant specificity is not due to a lack of other co-occurring AMF. Furthermore, despite the presence of ectomycorrhizal autotrophs throughout its geographical range, *Arachnitis* has not invaded the ectomycorrhizal mutualism as have other epiparasitic monocots (that is, orchids<sup>4,5</sup>). Instead, the arbuscular mycorrhizae-forming ancestors of *Arachnitis* reversed the direction of carbon flow entirely in their favour, and specialized on a narrow subset of AMF.

*Voyriella* and *Voyria* samples from tropical rainforests in French Guyana were also associated with a restricted set of closely related AMF. The intraradical morphology of the fungal symbionts of *Voyria* has been interpreted as a special form of arbuscular mycorrhiza<sup>1,15</sup>, but proof was lacking because arbuscules are not formed. We show that the AMF of *Voyriella* and most *Voyria* examined are from the same clade of *Glomus* as the AMF of *Arachnitis*. All AMF of *Voyriella* were from one narrow lineage within *Glomus* group A. Most AMF of *Voyria* (*V. aurantiaca*, *V. rosea*, *V. caerulea*, *V. corymbosa*, *V. tenuiflora*) formed a monophyletic lineage within *Glomus* group A (Fig. 2). The only exceptions were one *V. aurantiaca* root containing a symbiont related to *Glomus sinuosum* and a *V. tenuiflora* root with both *Gigaspora* and the *Glomus* we found in all the other *Voyria* species. The principal lineage associated with *Voyria* was also detected in adjacent photosynthetic plant roots, including roots near *Voyriella*. Furthermore, there was no symbiont overlap between *Voyria* and *Voyriella* at a site where they co-occurred. Therefore, as in ectomycorrhizal epiparasites<sup>4,6,7</sup>, the specificity observed is not based solely on local availability of susceptible fungi.

These are currently the only known examples of specialization by a plant for a phylogenetically restricted set of AMF. Parasites are generally more specialized than mutualists<sup>19</sup>, and accordingly both ectomycorrhizal and now arbuscular mycorrhizal epiparasites turn out to be more specialized than their photosynthetic counterparts. Epiparasitism is at the extreme end in a continuum of plant–fungal mycorrhizal interactions that ranges from parasitism of either partner to mutualistic interactions<sup>20,21</sup>. This suggests that we should look for evidence of inter-plant carbon transfer among pairs of green plants that have been found to differ in species-specific outcomes of AMF colonization<sup>22–25</sup>, as specialized myco-heterotrophy suggests that net flux of carbon from fungus to plant occurs within arbuscular mycorrhizal networks. □

## Methods

### *Arachnitis* fungi

We obtained eight plants of *Arachnitis uniflora* from three populations in Nahuel Huapi National Park (Río Negro province, Argentina): two from Lake Verde, one from Mount Otto, and five from the Llao-Llao area (41° 7.27' S, 71° 23.52' W). Lake Verde is approximately 75 km away from Llao-Llao, and Mount Otto is halfway between these two locations. The plants encompassed the morphological variation (that is, size and colour) observed at these sites and all produced an identical plant nrITS sequence (AF480089). For microscopy, *Arachnitis* roots were embedded (Kulzer Histo-Technique 7100), sectioned (4 µm) and stained with Cresyl blue, Cotton blue, Trypan blue, or iodine solution. The fungal structures are characteristic of vesicular arbuscular mycorrhizae and include intracellular bundles of 5–6 vesicles borne from a single hypha, coils, and relatively sparse arbuscules. When the flowering shoot develops, colonized cortical layers become completely lysed and only loosely arranged mycelium remains.

We also extracted genomic DNA from individual sections (~0.5 mm × 2 mm) of roots from each plant following methods described elsewhere<sup>26</sup>, with a purification step using GeneClean II (Q-Biogene). We amplified the fungal nrITS using the universal fungal primers ITS1F and ITS4 (refs 26, 27) and we sequenced 6–12 fungal nrITS clones from each plant (AF480093–AF480148). About 15% of these sequences were disregarded as they

were plant ITS sequences or sequences closely related to fungal lineages known to not form mycorrhizae (*Neurospora*, *Rhodoturula*, *Mortierella*). The complete 18S was cloned and sequenced from NS1 and GLOM5.8R<sup>27,28</sup> amplicons obtained from one plant from each location (AF480150–AF480158).

### Fungal symbionts of plants near *Arachnitis*

To test whether the *Arachnitis* mycorrhizal fungus is also present in roots of photosynthetic plants, we designed a primer specific to the symbiont (glomits1f: GCGTCCGTCATTATTT AAAACC). From 36 root fragments (5 mm long) collected near or attached to *Arachnitis* roots we extracted genomic DNA and amplified the nrITS with glomits1f and ITS4. Three root fragments amplified in the first round of PCR, and an additional four amplified after a second round using 10<sup>-2</sup> dilutions of the initial reactions. These amplicons were sequenced to confirm their identity as the *Arachnitis* symbiont (AF503648–AF503654). The genomic extracts of the roots were also used to amplify the plant nrITS using the primers ITS1 and ITS4. To assess some of the diversity of other AMF near *Arachnitis* roots, we applied a clade-specific nested PCR approach<sup>29</sup> to the same roots of photosynthetic plants used above and we found two different nuclear DNA sequences from *Glomus* groups A and B (AF480160, AF480161). In addition, a sporocarp with another nuclear ribosomal DNA sequence from *Glomus* group A (AF480159) was found less than 10 cm from one *Arachnitis*. These three sequences did not match the *Arachnitis* symbiont sequences and were too divergent for unambiguous alignment to the data set analysed in Fig. 1.

### *Voyria* and *Voyriella* fungi

We sampled three plants of *Voyriella parviflora*, two of *Voyria rosea*, two of *V. tenuiflora* and one of *V. corymbosa* from a site in central French Guyana (3° 40.4' N, 53° 12.5' E). One *V. caerulea* and two *V. aurantiaca* plants were sampled from another site about 10 km away. Genomic DNA was extracted using a Qiagen DNeasy mini kit. A nested PCR procedure described elsewhere<sup>28</sup> was used to amplify the nrITS and the 3'-terminal region of the 18S ribosomal DNA. The fungal symbionts were members of *Glomus* group A based on NS5 and GLOM5.8R PCR products, which were cloned, screened with *Hinf*I, and sequenced (AJ430854–AJ430858, AJ437204–AJ437208, AJ437210). In one case, a Gigasporaceae symbiont was identified using the primers NS5 and GIGA28R (AJ437216, GIGA28R: TTCAGCGGGTACTCTACA). In a subset of specimens the less specific primer AM1 (ref. 12) used in combination with NS3 (ref. 27) confirmed our results (AJ437211–AJ437215) and the absence of other AMF. Combinations of universal primers, AM1, and primers specific to *Glomus* group A (GLOM1070R<sup>29</sup>, GLOM5.8R<sup>28</sup>, GLOM1311R: GAAGCTGGCGACTAACA) were used to amplify and sequence the complete 18S of the two principal fungal symbionts (AJ430852, AJ430853). Most *Glomus* group A sequences obtained fell into two types: type 1 was detected in all plants of *Voyriella* and type 2 was found in all *Voyria* plants. A third type, related to *Glomus sinuosum*, was found in one plant of *V. aurantiaca*. The roots of other plants intermingled with those of *Voyria* and *Voyriella* were analysed by the same methods and type 2 sequences were detected (AJ437209, AJ438773). In addition, we designed primers specific to type 1 (voyM1660: TGTCAAGGGTCTTTGGTTGG) and type 2 (voyQ1660: ATTAGGACTGGMAACA GAC). Type 1 products were successfully amplified only from *Voyriella* and type 2 only from *Voyria*. These amplicons were screened by restriction analysis and their identity confirmed by sequencing (AJ437102, AJ437103).

### DNA sequence analysis

Nucleotide sequencing was performed on ABI 310 and ABI 3100 Genetic Analyzers using BigDye chemistry. Sequences were aligned manually into datasets of: (1) internal transcribed spacer sequences from symbionts and *Glomus* group A sequences from the database; (2) partial 18S nuclear DNA sequences<sup>12</sup>; and (3) sequences of the complete 18S nuclear DNA of glomalean fungi and outgroups from the database. Data sets were analysed with PAUP\*4.0beta8 (ref. 30).

Received 15 March; accepted 19 July 2002; doi:10.1038/nature01054.

1. Leake, J. R. The biology of myco-heterotrophic ('saprophytic') plants. *New Phytol.* **127**, 171–216 (1994).
2. Björkman, E. *Monotropia hypopithys* L.—an epiparasite on tree roots. *Physiol. Plantarum* **13**, 308–327 (1960).
3. Cullings, K. W., Szaro, T. M. & Bruns, T. D. Evolution of extreme specialization within a lineage of ectomycorrhizal epiparasites. *Nature* **379**, 63–66 (1996).
4. Taylor, D. L. & Bruns, T. D. Independent, specialized invasions of ectomycorrhizal mutualism by two nonphotosynthetic orchids. *Proc. Natl Acad. Sci. USA* **94**, 4510–4515 (1997).
5. McKendrick, S. L., Leake, J. R. & Read, D. J. Symbiotic germination and development of myco-heterotrophic plants in nature: transfer of carbon from ectomycorrhizal *Salix repens* and *Betula pendula* to the orchid *Corallorhiza trifida* through shared hyphal connections. *New Phytol.* **145**, 539–548 (2000).
6. Bidartondo, M. I. & Bruns, T. D. Extreme specificity in epiparasitic Monotropoideae (Ericaceae): widespread phylogenetic and geographical structure. *Mol. Ecol.* **10**, 2285–2295 (2001).
7. Bidartondo, M. I. & Bruns, T. D. Fine-level mycorrhizal specificity in the Monotropoideae (Ericaceae): specificity for fungal species groups. *Mol. Ecol.* **11**, 557–569 (2002).
8. Molina, R., Massicotte, H. & Trappe, J. M. *Mycorrhizal Functioning* (ed. Allen, M. F.) 357–423 (Chapman & Hall, London, 1992).
9. Simard, S. W. *et al.* Net transfer of carbon between ectomycorrhizal tree species in the field. *Nature* **388**, 579–582 (1997).
10. Smith, S. E. & Read, D. J. *Mycorrhizal Symbiosis* (Academic, San Diego, 1997).
11. Helgason, T., Daniell, T. J., Husband, R., Fitter, A. H. & Young, J. P. W. Ploughing up the wood-wide web? *Nature* **394**, 431 (1998).
12. Helgason, T., Fitter, A. H. & Young, J. P. W. Molecular diversity of arbuscular mycorrhizal fungi colonising *Hyacinthoides non-scripta* (bluebell) in a seminatural woodland. *Mol. Ecol.* **8**, 659–666 (1999).

13. Fitter, A. H., Graves, J. D., Watkins, N. K., Robinson, D. & Scrimgeour, C. Carbon transfer between plants and its control in networks of arbuscular mycorrhizas. *Funct. Ecol.* **12**, 406–412 (1998).
14. Robinson, D. & Fitter, A. The magnitude and control of carbon transfer between plants linked by a common mycorrhizal network. *J. Exp. Bot.* **50**, 9–13 (1999).
15. Imhof, S. Root anatomy and mycotrophy of the achlorophyllous *Voyria tenella* Hook. (Gentianaceae). *Botanica Acta* **110**, 298–305 (1997).
16. Yamato, M. Identification of a mycorrhizal fungus in the roots of achlorophyllous *Sciaphila tosaensis* Makino (Triuridaceae). *Mycorrhiza* **11**, 83–88 (2001).
17. Schwarzott, D., Walker, C. & Schüßler, A. *Glomus*, the largest genus of the arbuscular mycorrhizal fungi (Glomales), is nonmonophyletic. *Mol. Phylogenet. Evol.* **21**, 190–197 (2001).
18. Lanfranco, L., Delpero, M. & Bonfante, P. Intraspecific variability of ribosomal sequences in the endomycorrhizal fungus *Gigaspora margarita*. *Mol. Ecol.* **8**, 37–45 (1999).
19. Price, P. W. *Evolutionary Biology of Parasites* (Princeton Univ. Press, Princeton, 1980).
20. Johnson, N. C., Graham, J. H. & Smith, F. A. Functioning and mycorrhizal associations along the mutualism-parasitism continuum. *New Phytol.* **135**, 575–586 (1997).
21. Smith, F. A. & Smith, S. E. Mutualism and parasitism: diversity in function and structure in the 'arbuscular' (VA) mycorrhizal symbiosis. *Adv. Bot. Res.* **22**, 1–43 (1996).
22. McGonigle, T. P. & Fitter, A. H. Ecological specificity of vesicular-arbuscular mycorrhizal associations. *Mycol. Res.* **94**, 120–122 (1990).
23. Johnson, N. C., Tilman, D. & Wedin, D. Plant and soil controls on mycorrhizal fungal communities. *Ecology* **73**, 2034–2042 (1992).
24. Bever, J. D., Morton, J. B., Antonovics, J. & Schultz, P. A. Host-dependent sporulation and species diversity of arbuscular mycorrhizal fungi in a mown grassland. *J. Ecol.* **84**, 71–82 (1996).
25. van Der Heijden, M. G. A. *et al.* Mycorrhizal fungal diversity determines plant biodiversity, ecosystem variability and productivity. *Nature* **396**, 69–72 (1998).
26. Gardes, M. & Bruns, T. D. ITS primers with enhanced specificity for basidiomycetes: application to the identification of mycorrhizae and rusts. *Mol. Ecol.* **2**, 113–118 (1993).
27. White, T. J., Bruns, T. D., Lee, S. & Taylor, J. W. *PCR Protocols: A Guide To Methods And Applications* (eds Innis, M. A., Gelfand, D. H., Sninsky, J. J. & White, T. J.) 315–322 (Academic, San Diego, 1990).
28. Redecker, D. Specific PCR primers to identify arbuscular mycorrhizal fungi within colonized roots. *Mycorrhiza* **10**, 73–80 (2000).
29. Redecker, D., Morton, J. B. & Bruns, T. D. Molecular phylogeny of the arbuscular mycorrhizal fungi *Glomus sinuosum* and *Sclerocystis coremioides*. *Mycologia* **92**, 282–285 (2000).
30. Swofford, D. L. *PAUP\*: Phylogenetic Analysis Using Parsimony* (Sinauer, Sunderland, Massachusetts, 2002).

## Acknowledgements

We thank I. Gamundí for an *Arachnitis* sample, B. Giménez for help in locating *Arachnitis* populations, T. Szaro for computer assistance, and T. Boller and D. Hibbett for comments on the manuscript. This work was supported by the National Science Foundation and the Royal Society of London.

## Competing interests statement

The authors declare that they have no competing financial interests.

Correspondence and requests for materials should be addressed to M.I.B. (e-mail: martinb@nature.berkeley.edu).

# RGM is a repulsive guidance molecule for retinal axons

Philippe P. Monnier\*†, Ana Sierra\*†, Paolo Macchi‡, Lutz Deitinghoff\*, Jens S. Andersen§, Matthias Mann§, Manuela Flad||, Martin R. Hornberger\*, Bernd Stahl\*, Friedrich Bonhoeffer‡ & Bernhard K. Mueller\*

\* Migragen AG, Spemannstraße 34, 72076 Tuebingen, Germany

‡ Max-Planck-Institut für Entwicklungsbiologie, Spemannstraße 35, 72076 Tuebingen, Germany

§ Department of Biochemistry and Molecular Biology, University of Southern Denmark, Campusvej 55, 5230 Odense M, Denmark

|| DeveloGen AG, 37079 Goettingen, Germany

† These authors contributed equally to this work

**Axons rely on guidance cues to reach remote targets during nervous system development<sup>1</sup>. A well-studied model system for axon guidance is the retinotectal projection. The retina can be divided into halves; the nasal half, next to the nose, and the temporal half. A subset of retinal axons, those from the temporal half, is guided by repulsive cues expressed in a graded fashion in**

**the optic tectum<sup>2,3</sup>, part of the midbrain. Here we report the cloning and functional characterization of a membrane-associated glycoprotein, which we call RGM (repulsive guidance molecule). This molecule shares no sequence homology with known guidance cues, and its messenger RNA is distributed in a gradient with increasing concentration from the anterior to posterior pole of the embryonic tectum. Recombinant RGM at low nanomolar concentration induces collapse of temporal but not of nasal growth cones and guides temporal retinal axons *in vitro*, demonstrating its repulsive and axon-specific guiding activity.**

The retinotectal map is characterized by a precise mapping of retinal ganglion cells to the optic tectum so that their terminations form a reversed image of the retina<sup>2</sup>. The temporal half of the retina projects to the anterior part of the optic tectum, and the nasal retina to the posterior tectum<sup>2</sup>. Glycosylphosphatidylinositol (GPI)-linked molecules have been proposed to be important in guiding temporal retinal axons to their correct topographic position in the optic tectum by repelling this axon class from the posterior part of the tectum<sup>3</sup>. Efforts to identify these guidance cues led to ephrins<sup>4,5</sup> (that is, ligands of Eph receptor tyrosine kinases), and to a GPI-anchored glycoprotein that had a relative molecular mass of 33,000 ( $M_r$  33K) and an isoelectric point of approximately 8 (ref. 6).

On the basis of these characteristics, we purified a protein from tectal membranes of embryonic chicken, and analysed it by nano-electrospray mass spectrometry. Subsequent screening of a complementary DNA library from embryonic chicken with a probe derived from the resulting amino-acid sequences retrieved a cDNA of 1,486 nucleotides (Fig. 1a). The protein encoded consists of 432 residues; it covered 9 out of ten sequence stretches obtained from mass spectrometry (Fig. 1a). The methionine indicated in Fig. 1a probably defines the translation start of RGM as it is preceded by a Kozak sequence<sup>7</sup>. Surprisingly, the predicted relative molecular mass for a protein with 432 residues is much higher than 33K. Indeed, an amino-terminal sequence determination using Edman degradation resulted in the amino-acid sequence PHLRT, strongly suggesting that native RGM starts with residue 150 (Fig. 1a).

Sequence analysis showed that RGM has no significant homology to any other known guidance molecule. As predicted by the hydrophobicity profile using the Kyte and Doolittle algorithm<sup>8</sup>, RGM contains two hydrophobic domains at the N and carboxy terminus (Fig. 1b, c). The N-terminal domain seems to represent a conventional signal peptide, whereas the C-terminal domain is a GPI-anchor domain, in agreement with the characterization of RGM as a GPI-anchored plasma membrane protein<sup>6</sup>. Moreover, there is a tri-amino-acid motif, the RGD site<sup>9</sup>, which could be involved in cell attachment, and a partial von Willebrand factor type D domain<sup>10</sup>. Most of its key amino acids are present in RGM. Nevertheless, it is only a partial domain, comprising about 40% of a full-length domain<sup>10</sup>.

We investigated the distribution of RGM message and protein expression by *in situ* hybridization and antibody staining. *In situ* hybridization with an RGM-specific anti-sense probe on cryostat sagittal sections from chicken tecta (E9) showed strong staining in the periventricular layer surrounding the tectal ventricle (Fig. 2a). The staining intensity observed with an RGM anti-sense probe is much stronger in posterior than anterior tectum. This staining gradually increases from the anterior to posterior pole, suggesting that RGM mRNA forms a spatial gradient along the anterior-posterior axis of the embryonic chicken tectum. DAPI staining of the nuclei revealed that the cell density in the periventricular layer is almost constant along the anterior-posterior axis (Fig. 2b). This finding implies that the gradient is formed by a different degree of expression rather than by a different density of cells expressing RGM mRNA.

The polyclonal antibody raised against chicken RGM specifically recognized a single protein of  $M_r$  33K on western blots (Fig. 2c). To